Vol. 22, No. 3(2023) Alim2386
Revista Mexicana de Ingeniería Química

Optimizing foam mat drying process for cornelian cherry pulp using response surface methodology and artificial neural networks

Optimización del proceso de secado de la pulpa de cereza cornalina mediante la metodología de superficie de respuesta y redes neuronales artificiales

M. Güldane*
Program of Laboratory Technology, Pamukova Vocational School, Sakarya University of Applied Sciences, Sakarya, Turkey.
Received: July 6, 2023; Accepted: August 28, 2023

Abstract
This study aimed to improve the foam mat drying (FMD) process of cornelian cherry pulp. Response surface methodology (RSM) and artificial neural networks (ANN) were employed to investigate and predict the impact of ultrasound treatment (10-30 min), whipping (5-15 min, and hot-air temperature (60-80 °C) on selected responses. The results showed that maximum redness value and total phenolic content, and minimum drying time were obtained when optimum process parameters, 10 min for sonication time, 15 min for whipping time, and 60 °C for drying temperature, were employed. Analysis of variance (ANOVA) results indicated that the most important parameter influencing the FMD process of cornelian cherry pulp was the drying temperature. Furthermore, the statistical comparison of the empirical and predictive results for each response showed that the ANN model has a better prediction capability than the RSM. The overall findings revealed that the ANN model can be successfully applied in predicting responses in FMD of valuable fruits.
Keywords: ANOVA, drying temperature, prediction, ultrasound, whipping.

Resumen
El objetivo de este estudio era mejorar el proceso de secado de espuma (FMD) de la pulpa de cereza cornalina. Se emplearon la metodología de superficie de respuesta (RSM) y las redes neuronales artificiales (ANN) para investigar y predecir el impacto del tratamiento con ultrasonidos (10-30 min), el batido (5-15 min) y la temperatura del aire caliente (60-80 °C) sobre las respuestas seleccionadas. Los resultados mostraron que el máximo enrojecimiento y contenido fenólico total y el mínimo tiempo de secado se obtuvieron cuando se emplearon los parámetros óptimos del proceso, 10 min para el tiempo de sonicación, 15 min para el tiempo de batido y 60 °C para la temperatura de secado. Los resultados del análisis de la varianza (ANOVA) indicaron que el parámetro más importante que influye en el proceso de FMD de la pulpa de cereza cornalina es la temperatura de secado. Además, la comparación estadística de los resultados empíricos y predictivos para cada respuesta mostró que el modelo ANN tiene una mejor capacidad de predicción que el RSM. Los resultados globales revelaron que el modelo RNA puede aplicarse con éxito en la predicción de respuestas en la FMD de frutas valiosas.
Palabras clave: ANOVA, temperatura de secado, predicción, ultrasonidos, batido.

* *Corresponding author. E-mail*: mehmetguldane@subu.edu.tr;
https://doi.org/10.24275/rmiq/Alim2386
ISSN:1665-2738, *issn-e*: 2395-8472

1 Introduction

Cornelian cherry (*Cornus mas* L.) is a plant species belonging to the dogwood family, widely grown in countries such as Armenia, Georgia, Ukraine, Poland, and Turkey. Recent studies have revealed that this fruit is rich in bioactive substances including anthocyanins, flavanols, organic acids, and phenolics (Cosmulescu *et al*., 2019). Therefore, it is used in folk medicine for the treatment of certain diseases and in food processing to produce value-added products (Dupak *et al*., 2020). One of the most important disadvantages of cornelian cherry fruit is that it cannot maintain its freshness for a long time after harvesting due to its delicate texture. For this reason, it is usually further processed into various products after harvest (Vakula *et al*., 2019). Both fresh and dried cornelian cherries are used to manufacture value-added products including fruit preserves like jam, jelly, and marmalade, alcoholic (beer, wine, liqueur, etc.), and non-alcoholic (fruit juices, extracts, and concentrates, etc.) beverages and dairy products, including yogurt, cheese, and ice cream thanks to their functional coloring and flavoring properties(Parveez Zia & Alibas, 2021).

Drying has been the most widespread technique of preserving food materials since ancient times. The drying process reduces the moisture content to 1-5% and limits enzymatic and microbiological activities. The hot-air drying method has been extensively utilized in the food drying industry (Uslu Demir *et al*., 2019). Conventional drying reduced the drying time by increasing the dehydration temperature, but slower drying and prolonged exposure to oxygen can lead to the breakdown of bioactive components (Zielinska *et al*., 2017). Various dehydration techniques such as spray drying, tray drying, freeze drying, foam mat drying (FMD), and microwave drying are used to produce powdered products by drying fruit and vegetable juices, pulp, and puree (Varhan *et al*., 2019). FMD is a simple and relatively new drying technique preferred to remove excess moisture from food materials in order to increase their shelf life (Brar *et al*., 2020). FMD is a simple and relatively new drying technique to remove excess moisture from fruits and vegetables to extend their shelf life (Brar *et al*., 2020). Compared to conventional drying, it provides faster drying at lower temperatures and reduces energy consumption, therefore caused to minimize drying costs. Moreover, the suitability for food items sensitive to high temperatures and the potential to preserve bioactive components in the product during dehydration make FMD a valuable technique (Benkovic *et al*., 2019; Khodifad & Kumar, 2020).

The foaming properties of the juice or pulp have a considerable influence on the drying properties and thus on the quality characteristics of the powder produced through the FMD method. Studies have shown that the interactions between proteins and other components such as gums, sugars, and salts in a foam system are important in determining foam properties (Guldane & Dogan, 2022; Mohanan *et al*., 2020). However, recently, researchers have focused on improving foam properties. In these studies, it was emphasized that non-thermal processing methods improve foam quality characteristics including foam capacity and foam stability (Chen *et al*., 2019). Ultrasound affects the physicochemical composition of proteins and has a significant impact on their structural properties and thus interfacial behavior such as foaming and emulsifying (Mirmoghtadaie *et al*., 2016; Stefanović *et al*., 2017). This effect is known to be associated with cavitation and cavitation-related changes such as local based high temperature, high pressure, turbulence, dynamic agitation, and high shear force. Sonication has been reported to reduce the surface tension of protein solutions and increase protein adsorption at the interface between air and liquid phases, thereby improving foaming properties (Tan *et al*., 2015).

Optimization techniques such as response surface methodology (RSM), Taguchi method, principal component analysis, and artificial neural networks (ANN) are extensively utilized in the food industry to optimize production processes and predict response variables (Güldane, 2023; Guldane & Dogan, 2022). RSM is a set of statistical and mathematical approaches aimed at improving production efficiency (Šumić *et al*., 2016). In this technique, the optimal production conditions for the response characteristics are identified by analyzing the data obtained from the experiments performed based on certain experimental observations (Guarneros-Flores *et al*., 2019). Process optimization can only be achieved if the basic conditions of selecting the appropriate experimental design, estimating the response variable, and building mathematical models that represent the relationship between production parameters are provided (Bogusz *et al*., 2022). Being a relatively recent technique, The ANN is a deep learning method developed by simulating the ability of the human brain to solve a problem (Ameer *et al*., 2017). Neural networks are software programs designed to simulate and represent the relationship between process factors and targeted outputs. They can model complex, non-linear relationships directly from raw experimental data (Silva *et al*., 2020; Yadav *et al*., 2017). Limited research has been conducted on ANN modeling in the FMD process, including passion fruit (Samyor *et al*., 2021) and papaya (Qadri *et al*., 2020). To date, no studies have utilized these approaches to optimize process variables and predict response variables for the FMD of cornelian cherry. This work aims to

optimize the FMD process of cornelian cherry pulp and to predict the impact of process variables, such as sonication time, whipping time, and drying temperature, on drying characteristics, color attributes, and bioactive components using RSM and ANN models.

2 Materials and methods

2.1 Materials

Cornelian cherry fruits were purchased from a local store situated in Kütahya, Türkiye, and kept at 4 °C until analysis. Egg white powder and pectin samples were obtained from Tito, Türkiye. All the other chemicals and reagents were analytical grades and supplied by Merck, Germany.

2.2 Methods

2.2.1 Preparation of cornelian cherry pulp

The fruits were separated from the contaminating substances (stem, rotten fruits, etc.), washed, transferred to a clean muslin cloth, and removed the seeds by hand press. The concentrated pulp was diluted with distilled water and homogenized with a blender apparatus (Kenwood KM070, UK), and then the Brix value of the resulting diluted pulp was adjusted to 10 °Brix. The resulting pulps were stored in glass bottles at +4 °C until analysis.

2.2.2 Preparation of biopolymer solutions

The egg white (20% (w/v)) and pectin (2% (w/v)) solutions were stirred with a magnetic stirrer at a speed of 200 rpm until complete hydration was achieved. The gum solution was continuously stirred overnight, and the protein solution was stirred for 2 hours before being stored at +4 °C.

2.2.3 Foaming process

150 g of homogenized fruit pulp was weighed into a glass beaker, followed by the addition of 50 g of egg white and 50 g of pectin solutions. The resultant solution was agitated for 5 min with a magnetic stirrer at 200 rpm. Then, the pre-foaming solution was subjected to ultrasound treatment (CALISKAN LAB ULT 4045, China) for various times (10, 20, and 30 min). The resulting mixture was transferred to a mixing bowl of a planetary mixer (Kenwood KM070, England), with the temperature set to 50 °C and the rotation speed set to the lowest setting. The study conducted by Ibanoglu & Erçelebi (2007) indicated that moderate heat treatment of biopolymer solutions containing egg protein and pectin resulted in higher foaming capacity compared to those without heat treatment. Once the pre-foaming solution reached 50 °C, the mixer temperature was adjusted to 25 °C, and the rotation speed of the planetary mixer (Kenwood KM070, England) was set to 180 rpm. Finally, the solution was whipped for various periods of time (5, 10, and 15 min) to obtain cornelian cherry foam.

2.2.4 Drying procedure

The resulting foam was poured onto a rectangular aluminum tray (width: 10 cm, length: 20 cm, and height: 2 cm) and uniformly spread to a height of 0.5 cm using a plastic spatula. The sample was then placed in a laboratory tray drier designed by Çelik Kardeler Ltd. Com. (Sakarya, Türkiye). The dryer was equipped with digital controls to adjust and monitor the temperature and relative humidity. The dryer had a stainless steels body with external insulation and had external dimensions of 70 × 55 × 55 cm and internal dimensions of 40 × 40 × 45 cm. The temperature control system had a working range of 40-120 ºC, while the air velocity system had a working range of 0-2 m/s. Each sample was dried at an air velocity of 1 m/s and three hot-air temperatures (60 °C, 70 °C, and 80 °C). Throughout the drying, the tray was weighed with an electronic scale (Radwag PS 4500, Poland) at 10 min intervals. The dehydration process was continued till the target moisture content below 5% (wet basis (w.b)). The moisture level of dried powders was measured with an infrared moisture meter (IR-60, Denver Instrument, Bohemia, NY). The drying time of the cornelian cherry foam was recorded in min. After drying, the dehydrated foam was cooled and scrapped with a spatula, and ground for 1 min using a coffee grinder. The powders were sieved through a 200 μm mesh sieve, then immediately packaged in high-density polypropylene bags and sealed to prevent air diffusion.

2.2.5 RSM modeling

A three-factor three-level BBD was conducted using Design Expert software (ver. 13.0, Stat-Ease Co., Minneapolis, MN, USA). The study investigated the impact of sonication time (X_1= 10-30 min), whipping time (X_2= 5-15 min), and drying temperature (X_3= 60-80 °C) on drying time, redness, and TPC. The experimental design included 15 experiments with 3 replicates at the center point, as shown in Table 1. Experimental runs were randomly performed to minimize the impact of unexpected changes in the responses. The three process variables, X_1, X_2, and X_3 were coded into three levels (+1, 0, and -1) to represent high, middle, and low values, respectively. The variables were coded using Eq. (1):

$$x_i = \frac{X_i - X_0}{\Delta X}, \quad i = 1,2,3,\ldots \tag{1}$$

Table 1. The actual and coded levels of process variables, experimental, and predicted results.

	Process parameters			Experimental results			RSM predicted			ANN predicted		
Run	X_1	X_2	X_3	Y_1	Y_2	Y_3	Y_1	Y_2	Y_3	Y_1	Y_2	Y_3
1	20(0)	5(-1)	60(-1)	95	23.73	121.73	90	23.42	120.65	90	23.55	120.65
2	20(0)	10(0)	70(0)	55	22.91	107.71	55.38	22.97	107.22	55	23.35	107.59
3	30(+1)	10(0)	80(+1)	60	22.27	103.64	57.88	22.25	102.78	60	22.27	102.78
4	30(+1)	15(+1)	70(0)	90	23.37	116.22	90	23.42	120.65	90	23.55	118.65
5	10(-1)	10(0)	60(-1)	60	23.26	110.25	58.75	23.24	111.42	60	23.26	111.42
6	10(-1)	5(-1)	70(0)	82	24.88	155.88	79	24.99	155.71	82	24.88	155.1
7	20(0)	10(0)	70(0)	90	25.14	130.12	89.63	24.99	130.61	88.29	25.36	130.61
8	10(-1)	15(+1)	70(0)	80	23.54	131.03	82.13	23.47	131.89	80	23.61	131.89
9	20(0)	15(+1)	80(+1)	60	21.7	115.2	63	21.98	115.37	60	21.7	115.37
10	10(-1)	10(0)	80(+1)	100	23.04	124.77	101.25	23.46	123.59	100	23.04	123.59
11	30(+1)	5(-1)	70(0)	70	24.01	122.01	70.88	24.12	120.07	75.82	24.01	120.07
12	30(+1)	10(0)	60(-1)	70	24.11	113.23	73.38	24.21	111.57	70	24.11	111.57
13	20(0)	15(+1)	60(-1)	85	22.7	101.4	81.63	22.41	101.53	85	22.7	101.53
14	20(0)	5(-1)	80(+1)	85	23.4	124.09	90	23.42	120.65	90	23.55	120.65
15	20(0)	10(0)	70(0)	90	23.23	103.71	89.13	23.03	104.12	90	23.23	104.12

where x_i represents the coded value of a process parameter, X_i refers to the actual value of a process parameter, X_0 is the process parameter of the actual value at the central point, and ΔX is the step change value.

The response variables were modeled using a second-order polynomial equation (Eq. (2)), commonly used to represent the relationship between the responses and the process variables (Šumić *et al*., 2016).

$$Y = \beta_0 + \sum_{i=1}^{2} \beta_i X_i + \sum_{i=1}^{2} \beta_i X_i^2 + \sum_{i<j=1}^{2} \beta_{ij} X_i X_j \qquad (2)$$

where Y indicates the dependent variable, X_i and X_j are the production parameters, and the regression coefficients (b_0, b_i, b_{ij}, and b_{ii}) in the equation represent the intercept, linear, interaction, and quadratic terms, respectively. The statistical analysis was performed using Design Expert software, which generated three-dimensional surface response plots based on the polynomial equation derived from the data. These graphs were used to illustrate the relationship between the response and the process variables. The significance of each model was assessed using analysis of variance (ANOVA), and the statistical significance of the linear, quadratic, and interaction terms was analyzed using Fisher's F-test and *p*-values. The accuracy of each model was evaluated using the coefficient of determination (R^2) value, as well as the lack-of-fit test.

2.2.6 *ANN modeling*

The Neural Network Toolbox ("nntool") of MATLAB 2015a software was used to perform ANN modeling. The ANN estimated the non-linear relationship between FMD parameters and output variables using the same datasets that were used to develop the RSM model. A three-layer feed-forward neural network model was built (Fig. 1) and tested with the data from a total of 15 experiments. The data was divided into three sets: training (70%), testing (15%), and validation (15%). The experimental datasets were trained using a network architecture that consisted of an input layer with three neurons (sonication time (X_1), whipping time (X_2), and drying temperature (X_3)), an output layer with three neurons (drying time (Y_1), redness (Y_2), and TPC (Y_3)), and a hidden layer with a hyperbolic tangent sigmoid activation function (tansig). Selecting the appropriate number of neurons in the hidden layer is essential for the prediction ability of the ANN. In this study, the optimal network topology (3:n:1) was selected by "trial and error" (Dhurve *et al*., 2022). The number of neurons in the hidden layer varied from 1 to 15 to minimize the deviations between the predicted and observed values (Ameer *et al*., 2017). To train the ANN, the Levenberg-Marquardt backpropagation method was used as the learning algorithm. This iterative method enables to find the minimum of a multivariate function expressed as the sum of squares of nonlinear real-valued functions (Calderón-Ramírez *et al*., 2022). The developed ANN models were evaluated based on their mean square error (MSE, Eq. (3)) and correlation coefficient (R^2, Eq. (4)) values, where a lower MSE and higher R^2 indicate a better-fit model. The best-fit model was determined based on these criteria.

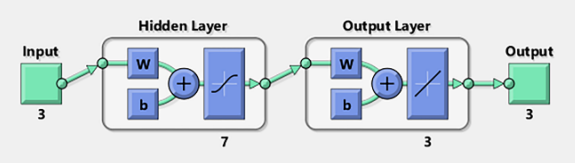

Fig. 1. Basic structure of the artificial neural network (ANN) model.

2.2.7 *Analysis of developed models*

Both RSM and ANN models were validated by using various statistical metrics such as MSE, R^2, mean absolute error (MAE), root mean square error (RMSE), and Chi-square (χ^2) (Eqs. (3)-(7)). These performance measures were used to compare the two models. A well-fitted model is characterized by lower MSE, MAE, RMSE, and χ^2 values, and higher R^2 values (Ajesh Kumar *et al*., 2022).

$$MSE = \frac{1}{n}\sum_{i=1}^{n}(y_i - y_{di})^2 \tag{3}$$

$$R^2 = 1 - \frac{\sum_{i=1}^{n}(y_i - y_{di})^2}{\sum_{i=1}^{n}(y_i - y_m)^2} \tag{4}$$

$$MAE = \frac{1}{n}\sum_{i=1}^{n}|(y_i - y_{di})| \tag{5}$$

$$RMSE = \sqrt{\frac{\sum_{i=1}^{n}(y_i - y_{di})^2}{2}} \tag{6}$$

$$\chi^2 = \sum_{i=1}^{n}\frac{(y_i - y_{di})^2}{y_i} \tag{7}$$

where n is the number of observations and y_i, y_{di}, and y_m are the observed, predicted, and mean observed values, respectively.

2.2.8 *Analysis*

2.2.8.1 Drying time

The drying time for each sample was considered as the time at which the moisture level of the final product reached below 5% (w.b).

2.2.8.2 Redness

The redness (a*+) of foam mat-dried cornelian cherry powder was determined by direct reading with a colorimeter (3nh, NR60CP, China) and the readings were reported using the Hunter Lab color scale.

2.2.8.3 Total phenolic content (TPC)

The total phenolic content (TPC) of the powders was determined according to the modified Folin-Ciocalteu reagent (FCR) method (Michalska-Ciechanowska *et al*., 2020). Briefly, 1 g of powder was mixed with 25 ml of 80% (v/v) methanol, agitated at 400 rpm for 15 min. The mixture was then centrifuged (K242R, Centurion Scientific, England) for 15 min at 5000 rpm, and the resulting supernatant was used to determine the TPC in foam mat-dried samples. 100 μl of the methanolic extract was mixed with 200 μl of FCR and 2 ml of distilled water in a test tube, followed by the addition of 1 ml of NaCO3 solution (20%) after 3 min. The reaction was allowed to proceed for 60 min in the dark and the absorbance of the specimen was measured at 765 nm using a UV/VIS spectrophotometer (Shimadzu UV-1240, Japan). The results were expressed as mg GAE/100 g powder dry matter (DM).

3 Results and discussion

3.1 *Model fitting*

A series of 15 experiments were conducted using BBD, involving three levels of process variables: sonication time, whipping time, and drying temperature, with the experimental results for response variables such as drying time, redness, and TPC shown in Table 1.

Table 2. ANOVA results for the RSM model.

Source	Drying time (Y_1)		Redness (Y_2)		TPC (Y_3)	
	F-value	p-value	F-value	p-value	F-value	p-value
Model	15.1	0.004*	26.87	$< 10^{-4}$*	38.97	0.0004*
X_1: Sonication time	2.39	0.183	4.76	0.0607	2.12	0.205
X_2: Whipping time	16.76	0.0094*	58.52	$< 10^{-4}$*	51.42	0.0008*
X_3: Drying temperature	81.68	0.0003*	78.18	$< 10^{-4}$*	178.8	$< 10^{-4}$*
X_1 X_2	0.2983	0.6084	0.6962	0.4283	3.99	0.1022
X_1 X_3	0.2983	0.6084	18.8	0.0025*	0.3236	0.594
X_2 X_3	3.87	0.1064	0.2619	0.6226	42.18	0.0013*
X_1 X_1	10.59	0.0226*	-	-	43.19	0.0012*
X_2 X_2	2.16	0.2017	-	-	0.5761	0.4821
X_3 X_3	21.33	0.0057*	-	-	23.06	0.0049*
Lack-of-fit	0.73	0.6221	1.83	0.394	0.1205	0.9401
R^2	0.9645		0.9527		0.9859	

* $p < 0.05$.

To evaluate the adequacy of the model, descriptive statistics such as the coefficient of determination (R^2) were examined, along with a lack-of-fit test that compares the disparities between the actual and predicted values to determine whether the relevant regression model fits the data. ANOVA data in Table 2 demonstrated that the proposed regression models are statistically significant for all responses, as evidenced by high F-values and low p-values ($p < 0.05$). A higher F-value and a p-value below 0.05 are considered desirable in model evaluation. The R^2 also provides information about the fitness of the generated models (Werede *et al*., 2021), with a higher R^2 value ($R^2 > 0.80$) generally indicating a reliable regression model (Meyabadi & Dadashian, 2012). Based on Table 3, the R^2 values of the drying time, redness, and TPC models are all above 0.90, indicating a strong correlation between the observed and predicted values. Furthermore, the lack-of-fit tests conducted on all response models suggest that there are no significant differences between the predicted and observed results ($p > 0.05$).

3.2 Effect of process variables on drying time (Y_1)

The impact of sonication time (X_1), whipping time (X_2), and drying temperature (X_3) on the drying characteristics of cornelian cherry pulp powders were studied, and the experimental findings for drying time are provided in Table 1. Drying time ranged from 55 to 100 min, indicating its dependence on the process parameters. The shortest drying time was observed at a sonication time of 10 min, a whipping time of 10 min, and a drying temperature of 80 °C, while the longest drying time was recorded at a sonication time of 20 min, the whipping time of 5 min, and drying temperature of 60 °C (Table 1). As seen, an increase in the drying temperature from 60 to 80 °C resulted in a decrease of about 63% in drying time.

The ANOVA results in Table 2 show the statistical significance of the linear, interaction, and quadratic terms. Whipping time (X_2) and drying temperature (X_3) were found to have a substantial influence on drying time, but sonication time (X_1) had no effect. However, all interaction terms were shown to have no impact on drying time ($p > 0.05$). Furthermore, Table 2 demonstrated that the quadratic effect of whipping time ($X_2\ X_2$) was not significant, whereas the quadratic effects of sonication time ($X_1\ X_1$) and drying temperature ($X_3\ X_3$) had a meaningful impact on drying time ($p < 0.05$). The quadratic equation (Eq. (8)), which includes the significant terms for the effects of process variables on drying time, is given as follows:

$$\text{Drying time}(Y_1) = 90 - 6.625X_2 - 14.625X_3 - 7.75X_1^2 - 11X_3^2 \quad (8)$$

The response surface graphs (Fig. 2a-c) depicted the influence of process variables, namely sonication time (X_1), whipping time (X_2), and drying temperature (X_3), on drying characteristics. Fig. 2a demonstrated that drying time decreased with an increase in whipping time at a constant sonication time (20 min). Notably, a substantial reduction (~20%) in drying time could be observed when whipping time increased from 5 min to 15 min. Increased whipping time enhanced the stability and foamability of the cornelian cherry foams, leading to a higher foaming capacity (data not shown). Mechanical whipping led to more air being entrapped in the continuous phase as the bubbles (Salahi *et al*., 2015). Moreover, an increment in whipping time resulted in the formation of smaller bubbles, which evenly distribute throughout the foam. Additionally, the stability could be increased by improving the viscoelastic properties of the interfacial lamella surrounding these bubbles (Ptaszek *et al*., 2014). Therefore, increasing the amount of air in the foam led to a widening of the effective area for the drying air and therefore to a faster diffusion of moisture in the structure. The quadratic effect of sonication time had a negative role in shortening the drying time (Eq. (8)). On the other hand, Fig. 2b shows that drying time increased with increasing sonication time from 10 to 20 min and then declined after reaching the middle level at a constant whipping time (10 min). This behavior may be attributed to the effect of sonication on the functionality of biopolymers. In foam systems, proteins can interact with other components to form aggregates with varying functional properties. The size of these aggregates can influence foaming capacity and foam stability (Mirmoghtadaie *et al*., 2016). These characteristics could be improved by adjusting the particle size with ultrasound treatment (Martínez-Padilla *et al*., 2015). Longer sonication times resulted in small-sized aggregates, leading to improved foaming properties (Stefanović *et al*., 2017). In this study, shorter drying times were achieved after 20 min of ultrasound treatment due to enhanced foaming properties. However, the effect of ultrasound treatment on drying time was found to be insignificant ($p > 0.05$) (Table 2). Fig. 2c demonstrated that the drying time for cornelian cherry foams decreased with an increase in drying temperature at a constant sonication time (20 min). This was attributed to the fact that higher drying temperatures reduced the internal resistance to water migration within the product. The relationship between drying temperature and vapor pressure gradient, molecular agitation, and the rate of water evaporation directly affected

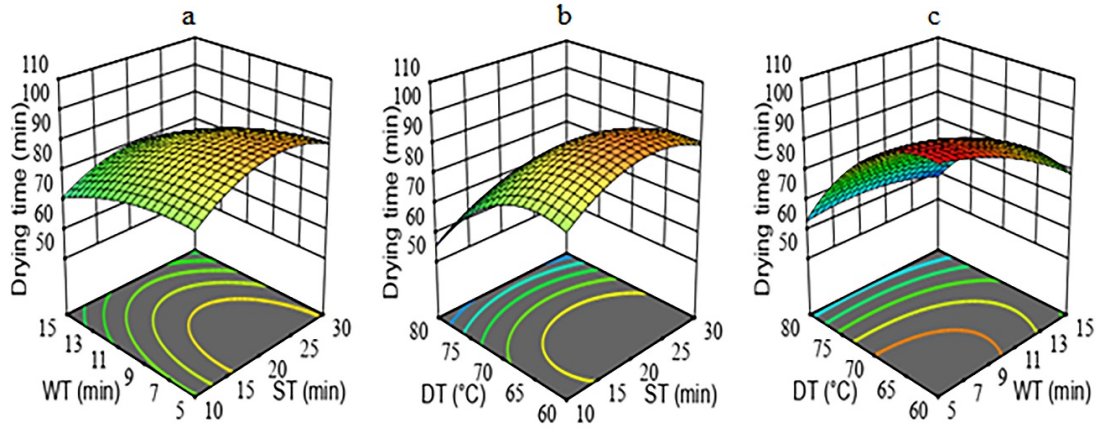

Fig. 2. Response surface plots for drying time (ST (min): sonication time; WT (min): whipping time; DT (°C): drying temperature).

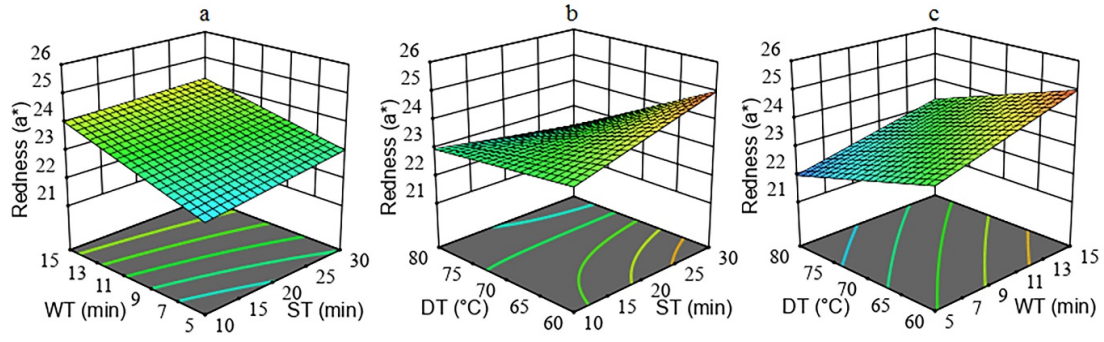

Fig. 3. Response surface plots for redness (ST (min): sonication time; WT (min): whipping time; DT (°C): drying temperature).

the drying process (Macedo *et al*., 2021). As the dehydration temperature increased, water evaporated more rapidly from the foamy structure, resulting in shorter drying times (Zheng *et al*., 2011). Similar trends have been observed in studies on collard green powder (Borges *et al*., 2022) and magenta leaves powder (Thuy *et al*., 2022). It is worth noting that there was no significant decrease in drying time when the temperature increased from 60 °C to 70 °C, while higher temperatures (> 70 °C) significantly increased the drying rate. Overall, the response surface graphs (Fig. 2 a-c) highlighted the complex relationships between the process variables and drying characteristics, emphasizing the importance of whipping time, sonication time, and drying temperature in optimizing the drying process of cornelian cherry foams.

3.3 Effect of process variables on redness (Y_2)

The variations in redness associated with the process variables are depicted in Table 1. The average values of redness varied between 21.69 and 25.14. The statistical analysis in Table 2 revealed that the linear terms of whipping time and drying temperature, as well as the interaction terms of sonication time and drying temperature, had a meaningful ($p < 0.05$) impact on the redness of the cornelian cherry powders. However, the linear term of sonication time (X_1) and the interaction terms of sonication time and whipping time (X_1 X_2) and whipping time and drying temperature (X_2 X_3) did not alter the color of the fruit powders. To describe the association between the process parameters and observed results, a second-order polynomial equation with interaction terms was developed using multiple regression analysis of the experimental data (Bozaci, 2019). Thus, the mathematical relation between redness (Y_2) and process factors (X_1, X_2, and X_3) can be expressed using Equation (9).

$$Redness\ (Y_2) = 23.42 + 0.70X_2 - 0.81X_3 - 0.56X_1X_3 \quad (9)$$

The influence of process variables on the color attributes of cornelian cherry foam powder was investigated. Three-dimensional surface plots (Fig. 3a-c) were generated to illustrate the correlation between sonication time (X_1), whipping time (X_2), and drying temperature (X_3). The contour plots displayed that drying temperature was the most important variable for the redness of the cornelian cherry powder. The

finding was also supported by ANOVA results in Table 2. Furthermore, the coefficient value for drying temperature in Eq (9) was the highest, indicating its dominant role in determining the redness of the powder. Based on the experimental data, increasing the drying temperature from 60 to 80 °C led to a 13% decrease in redness value (from 24.87 to 21.69) for cornelian cherry powders (Table 1). Fig. 3c further demonstrated that redness (a*) decreased with increasing hot-air temperature, primarily due to the thermal degradation of anthocyanins, which are responsible for the red color of the powder (Parveez Zia & Alibas, 2021). Similar observations on anthocyanin reduction with increasing temperature have been reported in foam mat-dried blueberry powder (Gao *et al*., 2022) and cornelian cherry drying (Aktas & Tontul, 2021).

Whipping time also played a significant role in determining redness (Eq. (9)). As depicted in Fig. 3a, the redness value increased with the mechanical whipping of cornelian cherry foams at a constant drying temperature (70 °C). Increasing whipping time from 5 to 15 min resulted in an increase in redness value from 21.69 to 25.14, respectively (Table 1). This enhancement in redness could be attributed to the improved foam properties, leading to an increased moisture diffusion rate throughout the drying process (Santos *et al*., 2022). The incorporation of air bubbles during the whipping process increased the foam porosity and thus facilitated moisture removal during drying (Osama *et al*., 2022).

The interaction term of sonication time and drying temperature (X_1 X_3) had a negative impact on the color of the cornelian cherry powders (Eq. (9)). Fig. 3b demonstrated that the redness of the sample powders decreased with increasing drying temperatures and decreasing sonication times at a constant whipping time (10 min). This decline could be attributed to the degradation of anthocyanins at higher temperatures and the limited release of color pigments due to the short-term application of ultrasound (Salacheep *et al*., 2020). However, the highest (25.14) and the lowest (22.91) values of redness for the powders were obtained when the drying temperature and sonication time were selected as 60 °C for 30 min and 80 °C for 10 min, respectively (Table 1).

3.4 Effect of process variables on total phenolic content (Y_3)

Experimental results for TPC (Y_3) of cornelian cherry foam powder under different FMD conditions, including sonication time (X_1), whipping time (X_2), and drying temperature (X_3) are presented in Table 1. The TPC values ranged from 101.39 to 155.88 mg GAE/100 g powder DM, indicating their dependence on the process variables. The highest TPC was obtained at a sonication time of 20 min, a whipping time of 15 min, and a drying temperature of 60 °C, while the lowest TPC was observed at a sonication time of 10 min, a whipping time of 5 min, and drying temperature of 70 °C. The ANOVA results revealed significant linear effects of whipping time (X_2) and drying temperature (X_3) on the bioactive content of cornelian cherry powder. Additionally, a statistically significant interaction between whipping time and drying temperature (X_2 X_3) and the quadratic effects of sonication time (X_1 X_1) and drying temperature (X_3 X_3) were observed (Table 2). A mathematical model describing the TPC of cornelian cherry foam powder, after excluding the insignificant terms, can be represented by Equation (10).

$$TPC(Y_3) = 120.68 + 7.04X_2 - 13.13X_3 - 9.02X_2X_3 - 9.50X_1^2 + 6.94X_3^2 \quad (10)$$

The impact of sonication time (X_1), whipping time (X_2), and drying temperature (X_3) on the TPC of cornelian cherry powder was analyzed using three-dimensional surface plots (Fig. 4a-c). The findings revealed that drying temperature had the most profound influence on TPC, as determined by Eq. (10). The linear and quadratic terms of drying temperature demonstrated that increasing hot-air temperature from 60 to 70 °C led to a reduction in TPC, whereas further increasing the temperature resulted in an increase in phenolic compounds. Similar findings were observed in the TPC variation of foam mat dried peaches (Brar *et al*., 2020) and hot-air convective dried blueberries (Zielinska *et al*., 2017). The increase in drying temperature may contribute to the formation of new phenolic compounds through the degradation of complex ones and/or reduce the loss of available phenolics by minimizing their exposure time to oxygen (Zielinska *et al*., 2017).

Whipping time also had a notable impact on TPC, as indicated by Eq. (10). Fig. 4a demonstrated that increasing the whipping time at a constant drying temperature (70 °C) caused an increase in TPC. The positive regression coefficient for whipping time (X_2) in Eq. (10) suggested that lower drying temperatures amplified the positive linear effect of the whipping time on TPC, probably due to reduced degradation of phenolic compounds. At a constant sonication time (20 min), Fig. 4c further showed that a significant negative interaction between whipping time and drying temperature could lead to a substantial improvement of about 35% in the TPC of cornelian cherry powder.

The quadratic effect of sonication time was found to be negatively correlated with TPC. Increasing ultrasound application from 10 to 20 min led to an increment in TPC, but further extending sonication time to 30 min significantly decreased TPC content.

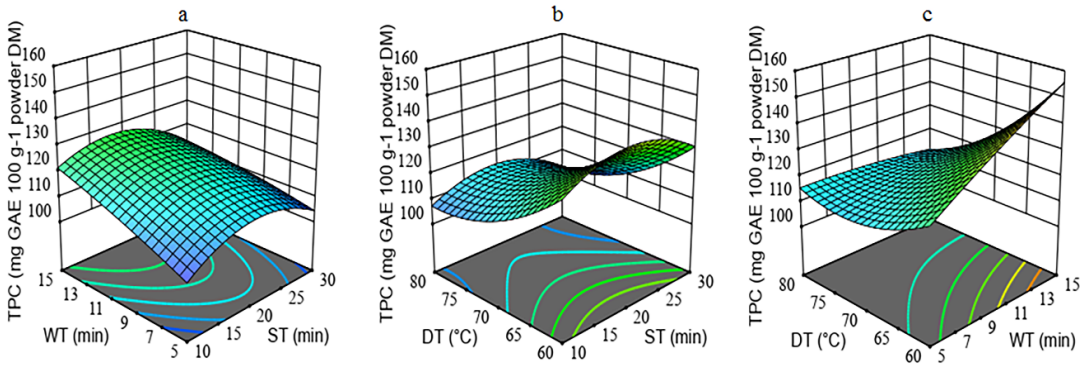

Fig. 4. Response surface plots for TPC (ST (min): sonication time; WT (min): whipping time; DT (°C): drying temperature).

This reduction could be attributed to a local increase in temperature caused by longer ultrasound treatment, leading to the degradation and structural destruction of phenolic components (Salacheep *et al*., 2020). Overall, the findings highlight the significant influence of drying temperature (X_3), whipping time (X_2), and sonication time (X_1) on the TPC of cornelian cherry powder, with specific interactions and quadratic effects playing important roles in determining the bioactive compounds.

3.5 Process optimization

The optimization of FMD conditions for cornelian cherry involved selecting the maximum redness value and TPC, and the minimum drying temperature as criteria. The desirability approach was employed for the numerical optimization of FMD conditions and to estimate the predicted responses. Through Design Expert software, with a desirability of 0.778, the optimal values for sonication, whipping time, and drying temperature were determined as 10 min, 15 min, and 60 °C, respectively. The resulting foam mat dried cornelian cherry powder produced under these conditions is presented in Fig. 5. The response values for optimal powder were predicted by the RSM model as 69 min for drying time, 24.34 for redness, and 149.63 mg GAE/100 g powder DM for TPC. These predicted values were also experimentally validated with three replications. The obtained results for drying time, redness, and TPC were 70 ± 0.00 min, 23.25 ± 0.06, and 145.33 ± 2.80 mg GAE/100 g powder DM, respectively. As a point, no statistical difference was observed between the predicted and experimentally validated response results at a 95% confidence interval.

The ANOVA results presented in Table 2 played a crucial role in the validation of the response surface models. The statistical analysis revealed that the drying time, redness, and TPC models were adequately accurate with higher R^2 ($R^2 > 0.95$) and lack of fit ($p > 0.05$) values. These results

Fig. 5. Foam mat dried cornelian cherry powder produced at optimal conditions.

demonstrated that RSM is a suitable and effective approach for optimizing the FMD process of cornelian cherry foam.

3.6 ANN modeling

ANN has been widely applied in solving engineering problems in recent years due to its self-learning and inference capabilities, allowing the ANN model to process random data and non-linear data. Malakar *et al*. (2022) used ANN to predict several responses, such as solid gain, weight loss, rehydration ratio, drying rate, and allicin content of garlic slices dried at an infrared drier. The values predicted by the ANN were close to the experimental results. Another study by Sharma *et al*. (2022) utilized ANN as an alternative to RSM to predict the cooking time, cooking losses, and water absorption ratio of fortified rice kernels. They found a close relationship between experimental findings and the values predicted by neural networks. Furthermore, moisture diffusion through cocoyam slices was successfully modeled using the ANN model

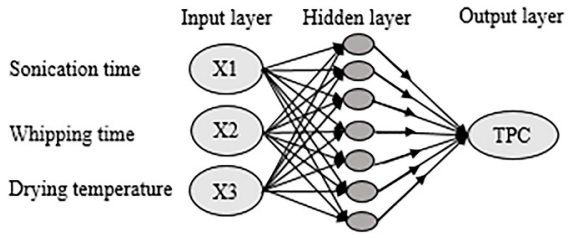

Fig. 6. ANN diagram for TPC response.

(Onu *et al*., 2021). Additionally, Anastácio *et al*. (2016) employed ANN for modeling the extraction process of phenolics from sweet potato peels, successfully predicting the TPC, ABTS, and DPPH of the extracts. These studies have demonstrated the successful application of the ANN model in the prediction of response variables.

ANN modeling was used to describe a non-linear correlation between process factors and targeted responses. A feed-forward backpropagation algorithm and topology optimization protocol were used to achieve this. The model was constructed using empirical datasets from the BBD matrix and consisted of one input layer with three neurons for sonication time, whipping time, and drying temperature, one hidden layer, and one output layer with three neurons for drying time, redness, and TPC. The tansig and purelin functions were used to connect the input and hidden layers and the hidden and output layer, respectively. The input layer received experimental data for a specific response variable and transmitted it to the hidden layer, which contained the optimal number of neurons. Data were processed with varied weights in these networks before being received by the output layer and transmitted to an external receiver (Nakhaei *et al*., 2017).

In this study, the dataset consisting of 15 experimental runs for each response was divided into three subsets: training (11 sets), validation (2 sets), and testing (2 sets). Levenberg-Marquardt algorithm was used to train the dataset using ANN (Yadav *et al*., 2017). For each response, the number of neurons in the hidden layer was determined statistically based on the lowest MSE and the highest R^2 values, which indicated the accuracy of the predictions made by the neural networks. Statistical results in Table 3 showed that the optimal number of neurons in the hidden layer was determined as 9, 9, and 7 for drying time, redness, and TPC responses, respectively. The general ANN topology for the TPC response is shown in Fig. 6. The MSE values for the optimal ANN topologies were calculated as 7.3409, 0.0693, and 0.6104 for the responses, respectively. In addition, the corresponding R^2 values are also higher than 0.98 (0.9841, 0.9971, and 0.9837, respectively), indicating a strong agreement between the observed results and the values predicted by the ANN (Table 1).

Table 3. Optimal network topologies and their corresponding statistical results.

Response	Network topology (3:n:1)	MSE	R^2
Drying time	9/3/01	7.3409	0.9841
Redness	9/3/01	0.0693	0.9971
TPC	7/3/01	0.6104	0.9837

3.7 Comparison of RSM and ANN models

A comparison was made between the estimation ability and prediction accuracy of RSM and ANN modeling approaches. The experimental data and also predicted values for the drying time, redness, and TPC obtained from both RSM and ANN models are tabulated in Table 1. It is evident from the overall results that, the predictions performed by the ANN model exhibit a significantly higher degree of agreement with the observed values, compared to the predictions provided by the RSM model. However, statistical characteristics such as MSE, R^2, MAE, RMSE, and χ^2 were used to evaluate and compare the model values, and the results are tabulated in Table 4.

It was observed that there were slight differences in the relevant response values obtained through ANN and RSM models. However, the ANN model exhibited higher accuracy in fitting the diverse data points compared to the RSM model. The superiority of the ANN model was evident from its higher R^2 value and lower values of MSE, MAE, RMSE, and χ^2. These results aligned with the conclusions drawn from previous studies on drying processes, which also highlighted the improved predictive capability of the ANN model (Malakar *et al*., 2022; Samyor *et al*., 2021). This advantage of the ANN model could be attributed to its ability to handle nonlinear systems, while the RSM model was more suitable for solving second-order polynomial regression problems (Kumar *et al*., 2022).

Conclusions

In this study, the foam mat drying process for cornelian cherry pulp was modeled and optimized. The influences of sonication time, whipping time, and drying temperature on the drying time, redness, and total phenolic content (TPC) were investigated. A response surface methodology based on a Box-Behnken design was employed to determine the optimal process conditions that maximize the redness and TPC while minimizing drying time. The RSM model successfully predicted the responses under optimal conditions, showing good agreement with the experimental results. On the other hand, the ANN model demonstrated superior predictive performance

Table 4. Statistical comparison of the results predicted by RSM and ANN models.

Response parameters	Response surface methodology (RSM)					Artificial neural networks (ANN)				
	MSE	R^2	MAE	RMSE	χ^2	MSE	R^2	MAE	RMSE	χ^2
Drying time	6.9833	0.9645	2.133	2.6426	1.3108	5.8042	0.9705	1.2	2.4092	1.078
Redness	0.0364	0.9517	0.1479	0.1909	0.0237	0.0222	0.9706	0.0825	0.149	0.0143
TPC	2.9433	0.9839	1.2331	1.7156	0.372	2.0526	0.9888	1.1157	1.4327	0.0423

compared to RSM. For all response variables, the ANN model exhibited higher determination coefficient (R^2) values and lower mean squared error (MSE), root mean squared error (RMSE), mean absolute error (MAE), and chi-square (χ^2) values. These findings contribute to the advancement of knowledge in modeling the foam mat drying process for commercially valuable fruits, emphasizing the potential of the ANN model in achieving accurate predictions for industrial applications.

Acknowledgment

References

Ajesh Kumar, V., Srivastav, P. P., Pravitha, M., Hasan, M., Mangaraj, S., V, P., & Verma, D. K. (2022). Comparative study on the optimization and characterization of soybean aqueous extract based composite film using response surface methodology (RSM) and artificial neural network (ANN). *Food Packaging and Shelf Life 31*, 100778. https://doi.org/10.1016/j.fpsl.2021.100778

Aktas, R. N., & Tontul, I. (2021). Usability of soapwort and horse chestnut saponin extracts as foaming agents in foam mat drying of pomegranate juice. *Journal of the Science of Food and Agriculture 101*(2), 786-793. https://doi.org/10.1002/jsfa.10770

Ameer, K., Bae, S. W., Jo, Y., Lee, H. G., Ameer, A., & Kwon, J. H. (2017). Optimization of microwave-assisted extraction of total extract, stevioside and rebaudioside-A from Stevia rebaudiana (Bertoni) leaves, using response surface methodology (RSM) and artificial neural network (ANN) modelling. *Food Chemistry 229*, 198-207. https://doi.org/10.1016/j.foodchem.2017.01.121

Anastácio, A., Silva, R., & Carvalho, I. S. (2016). Phenolics extraction from sweet potato peels: modelling and optimization by response surface modelling and artificial neural network. *Journal of Food Science and Technology 53*(12), 4117-4125. https://doi.org/10.1007/s13197-016-2354-1

Benković, M., Pižeta, M., Jurinjak Tušek, A., Jurina, T., Gajdoš Kljusurić, J., & Valinger, D. (2019). Optimization of the foam mat drying process for production of cocoa powder enriched with peppermint extract. *Lwt 115*, 108440. https://doi.org/10.1016/j.lwt.2019.108440

Bogusz, R., Wiktor, A., Nowacka, M., ćwintal, J., & Gondek, E. (2022). Foam-mat convective drying of kiwiberry (Actinidia arguta) pulp. *Czech Journal of Food Sciences 40*(3), 187-194. https://doi.org/10.17221/263/2020-CJFS

Borges, H. M. A., Borél, L. D. M. S., & Lima-Corrêa, R. A. B. (2022). Effects of temperature and foam layer thickness on collard greens powder production by foam mat drying. *Journal of Food Processing and Preservation 46*(8), 1-13. https://doi.org/10.1111/jfpp.16755

Bozaci, E. (2019). Optimization of the alternative treatment methods for *Ceiba pentandra* (L.) Gaertn (kapok) fiber using response surface methodology. *Journal of the Textile Institute 110*(10), 1404-1414. https://doi.org/10.1080/00405000.2019.1602897

Brar, A. S., Kaur, P., Kaur, G., Subramanian, J., Kumar, D., & Singh, A. (2020). Optimization of process parameters for foam-mat drying of peaches. *International Journal of Fruit Science 20*(S3), S1495-S1518. https://doi.org/10.1080/15538362.2020.1812017

Calderón-Ramírez, M., Gomez-Náfate, J. A., Ríos-Fuentes, B., Rico-Martínez, R., Martínez-Nolazco, J. J., & Botello-Álvarez, J. E. (2022). Analysis of the thermal efficiency of flat plate solar air heaters considering environmental conditions using artificial neural networks. *Revista Mexicana de Ingeniería Química 21*(3), Sim2833-Sim2833. https://doi.org/10.24275/rmiq/Sim2833

Chen, Y., Sheng, L., Gouda, M., & Ma, M. (2019). Impact of ultrasound treatment on the foaming and physicochemical properties of egg white during cold storage. *Lwt 113*(June), 108303. https://doi.org/10.1016/j.lwt.2019.108303

Cosmulescu, S., Trandafir, I., & Cornescu, F. (2019). Antioxidant capacity, total phenols, total flavonoids and colour component of cornelian cherry (*Cornus mas* L.) wild genotypes. *Notulae Botanicae Horti Agrobotanici Cluj-Napoca 47*(2), 390-394. https://doi.org/10.15835/nbha47111375

Dhurve, P., Suri, S., Malakar, S., & Arora, V. K. (2022). Multi-objective optimization of process parameters of a hybrid IR-vibro fluidized bed dryer using RSM-DF and RSM-GA for recovery of bioactive compounds from pumpkin seeds. *Biomass Conversion and Biorefinery*, 1-17. https://doi.org/10.1007/s13399-022-03151-3

Dupak, R., Jaszcza, K., Kalafova, A., Schneidgenova, M., Ivanisova, E., Tokarova, K., Brindza, J., & Capcarova, M. (2020). Characterization of compounds in Cornelian cherry (*Cornus mas* L.) and its effect on interior milieu in ZDF. *Emirates Journal of Food and Agriculture 32*(5), 368-375. https://doi.org/10.9755/ejfa.2020.v32.i5.2106

Gao, R., Xue, L., Zhang, Y., Liu, Y., Shen, L., & Zheng, X. (2022). Production of blueberry pulp powder by microwave-assisted foam-mat drying: Effects of formulations of foaming agents on drying characteristics and physicochemical properties. *Lwt 154*, 112811. https://doi.org/10.1016/j.lwt.2021.112811

Guarneros-Flores, J., Aguilar-Uscanga, M. G., Morales-Martínez, J. L., & López-Zamora, L. (2019). Maximization of fermentable sugar production from sweet sorghum bagasse (dry and wet bases) using response surface methodology (RSM). *Biomass Conversion and Biorefinery 9*(3), 633-639. https://doi.org/10.1007/s13399-018-00366-1

Güldane, M. (2023). Optimizing foam quality characteristics of model food using Taguchi-based fuzzy logic method. *Journal of Food Process Engineering*, e14384. https://doi.org/10.1111/jfpe.14384

Guldane, M., & Dogan, M. (2022). Multi-response optimization of process parameters of saponin-based model foam using Taguchi method and gray relational analysis coupled with principal component analysis. *Journal of Food Processing and Preservation 46*(5), 1-14. https://doi.org/10.1111/jfpp.16553

Ibanoglu, E., & Erçelebi, E. A. (2007). Thermal denaturation and functional properties of egg proteins in the presence of hydrocolloid gums. *Food Chemistry 101*(2), 626-633. https://doi.org/10.1016/j.foodchem.2006.01.056

Khodifad, B. C., & Kumar, N. (2020). Foaming properties of custard apple pulp and mathematical modelling of foam mat drying. *Journal of Food Science and Technology 57*(2), 526-536. https://doi.org/10.1007/s13197-019-04082-0

Kumar, G., Atif Wahid, M., Tanwar, P., & Kumar, M. (2022). Multi performance characteristics optimization of end milling parameters on surface quality and Micro-hardness of SS-304. *Materials Today: Proceedings 62*, 136-141. https://doi.org/10.1016/j.matpr.2022.02.608

Macedo, L. L., Corrêa, J. L. G., Araújo, C. da S., Vimercati, W. C., & Pio, L. A. S. (2021). Process optimization and ethanol use for obtaining white and red dragon fruit powder by foam mat drying. *Journal of Food Science 86*(2), 426-433. https://doi.org/10.1111/1750-3841.15585

Malakar, S., Dhurve, P., & Arora, V. K. (2022). Modeling and optimization of osmo-sonicated dehydration of garlic slices in a novel infrared dryer using artificial neural network and response surface methodology. *Journal of Food Process Engineering e14261*. https://doi.org/10.1111/jfpe.14261

Martínez-Padilla, L. P., García-Rivera, J. L., Romero-Arreola, V., & Casas-Alencáster, N. B. (2015). Effects of xanthan gum rheology on the foaming properties of whey protein concentrate. *Journal of Food Engineering 156*, 22-30. https://doi.org/10.1016/j.jfoodeng.2015.01.018

Meyabadi, T. F., & Dadashian, F. (2012). Optimization of enzymatic hydrolysis of waste cotton fibers for nanoparticles production using response surface methodology. *Fibers and Polymers 13*(3), 313-321. https://doi.org/10.1007/s12221-012-0313-7

Michalska-Ciechanowska, A., Majerska, J., Brzezowska, J., Wojdyło, A., & Figiel, A. (2020). The influence of maltodextrin and inulin on the physico-chemical properties of cranberry juice powders. *ChemEngineering 4*(1), 1-12. https://doi.org/10.3390/chemengineering4010012

Mirmoghtadaie, L., Shojaee Aliabadi, S., & Hosseini, S. M. (2016). Recent approaches in physical

modification of protein functionality. *Food Chemistry 199*, 619-627. https://doi.org/10.1016/j.foodchem.2015.12.067

Mohanan, A., Nickerson, M. T., & Ghosh, S. (2020). Utilization of pulse protein-xanthan gum complexes for foam stabilization: The effect of protein concentrate and isolate at various pH. *Food Chemistry 316*(January), 126282. https://doi.org/10.1016/j.foodchem.2020.126282

Nakhaei, M. R., Mostafapour, A., & Naderi, G. (2017). Optimization of mechanical properties of PP/EPDM/ clay nanocomposite fabricated by friction stir processing with response surface methodology and neural networks. *Polymer Composites 38*, E421-E432. https://doi.org/10.1002/pc.23942

Onu, C. E., Igbokwe, P. K., Nwabanne, J. T., & Ohale, P. E. (2022). ANFIS, ANN, and RSM modeling of moisture content reduction of cocoyam slices. *Journal of Food Processing and Preservation 46*(1), e16032. https://doi.org/10.1111/jfpp.16032

Osama, K., Younis, K., Qadri, O. S., Parveen, S., & Siddiqui, M. H. (2022). Development of under-utilized kadam (*Neolamarkia cadamba*) powder using foam mat drying. *Lwt 154*, 112782. https://doi.org/10.1016/j.lwt.2021.112782

Parveez Zia, M., & Alibas, I. (2021). The effect of different drying techniques on color parameters, ascorbic acid content, anthocyanin and antioxidant capacities of cornelian cherry. *Food Chemistry 364*(January), 130358. https://doi.org/10.1016/j.foodchem.2021.130358

Ptaszek, P., Zmudziński, D., Kruk, J., Kaczmarczyk, K., Roznowski, W., & Berski, W. (2014). The physical and linear viscoelastic properties of fresh wet foams based on egg white proteins and selected hydrocolloids. *Food Biophysics 9*(1), 76-87. https://doi.org/10.1007/s11483-013-9320-5

Qadri, O. S., Osama, K., & Srivastava, A. K. (2020). Foam mat drying of papaya using microwaves: Machine learning modeling. *Journal of Food Process Engineering 43*(6), e13394. https://doi.org/10.1111/jfpe.13394

Salacheep, S., Kasemsiri, P., Pongsa, U., Okhawilai, M., Chindaprasirt, P., & Hiziroglu, S. (2020). Optimization of ultrasound-assisted extraction of anthocyanins and bioactive compounds from butterfly pea petals using Taguchi method and Grey relational analysis. *Journal of Food Science and Technology 57*(10), 3720-3730. https://doi.org/10.1007/s13197-020-04404-7

Salahi, M. R., Mohebbi, M., & Taghizadeh, M. (2015). Foam-mat drying of cantaloupe (*Cucumis melo*): Optimization of foaming parameters and investigating drying characteristics. *Journal of Food Processing and Preservation 39*(6), 1798-1808. https://doi.org/10.1111/jfpp.12414

Samyor, D., Deka, S. C., & Das, A. B. (2021). Physicochemical and phytochemical properties of foam mat dried passion fruit (*Passiflora edulis* Sims) powder and comparison with fruit pulp. *Journal of Food Science and Technology 58*(2), 787-796. https://doi.org/10.1007/s13197-020-04596-y

Santos, N. C., Almeida, R. L. J., de Medeiros, M. de F. D., Hoskin, R. T., & da Silva Pedrini, M. R. (2022). Foaming characteristics and impact of ethanol pretreatment in drying behavior and physical characteristics for avocado pulp powder obtained by foam mat drying. *Journal of Food Science 87*(4), 1780-1795. https://doi.org/10.1111/1750-3841.16123

Sharma, A., Awasthi, A., Singh, T., Kumar, R., & Chauhan, R. (2022). Experimental investigation and optimization of potential parameters of discrete V down baffled solar thermal collector using hybrid Taguchi-TOPSIS method. *Applied Thermal Engineering 209*(September 2021), 118250. https://doi.org/10.1016/j.applthermaleng.2022.118250

Silva, L. K. R., Gonçalves, B. R. F., da Hora, F. F., Santos, L. S., & Ferrão, S. P. B. (2020). Spectroscopic method (FTIR-ATR) and chemometric tools to detect cow's milk addition to buffalo's milk. *Revista Mexicana de Ingeniería Química 19*(1), 11-20. https://doi.org/10.24275/rmiq/Alim560

Stefanović, A. B., Jovanović, J. R., Dojčinović, M. B., Lević, S. M., Nedović, V. A., Bugarski, B. M., & Knežević-Jugović, Z. D. (2017). Effect of the controlled high-intensity ultrasound on improving functionality and structural changes of egg white proteins. *Food and Bioprocess Technology 10*(7), 1224-1239. https://doi.org/10.1007/s11947-017-1884-5

Šumić, Z., Vakula, A., Tepić, A., Čakarević, J., Vitas, J., & Pavlić, B. (2016). Modeling and optimization of red currants vacuum drying

process by response surface methodology (RSM). *Food Chemistry 203*, 465-475. https://doi.org/10.1016/j.foodchem.2016.02.109

Tan, M. C., Chin, N. L., Yusof, Y. A., Taip, F. S., & Abdullah, J. (2015). Characterisation of improved foam aeration and rheological properties of ultrasonically treated whey protein suspension. *International Dairy Journal 43*, 7-14. https://doi.org/10.1016/j.idairyj.2014.09.013

Thuy, N. M., Tien, V. Q., Tai, N. Van, & Minh, V. Q. (2022). Effect of foaming conditions on foam properties and drying behavior of powder from magenta (*Peristrophe roxburghiana*) leaves extracts. *Horticulturae 8*(6), 546. https://doi.org/10.3390/horticulturae8060546

Uslu Demir, H., Atalay, D., & Erge, H. S. (2019). Kinetics of the changes in bio-active compounds, antioxidant capacity and color of Cornelian cherries dried at different temperatures. *Journal of Food Measurement and Characterization 13*(3), 2032-2040. https://doi.org/10.1007/s11694-019-00124-5

Vakula, A., Šumić, Z., Zeković, Z., Tepić Horecki, A., & Pavlić, B. (2019). Screening, influence analysis and optimization of ultrasound-assisted extraction parameters of cornelian cherries (*Cornus mas* L.). *Journal of Food Processing and Preservation 43*(12), 1-14. https://doi.org/10.1111/jfpp.14226

Varhan, E., Elmas, F., & Koç, M. (2019). Foam mat drying of fig fruit: Optimization of foam composition and physicochemical properties of fig powder. *Journal of Food Process Engineering 42*(4), 1-13. https://doi.org/10.1111/jfpe.13022

Werede, E., Jabasingh, S. A., Demsash, H. D., Jaya, N., & Gebrehiwot, G. (2021). Eco-friendly cotton fabric dyeing using a green, sustainable natural dye from Gunda Gundo (*Citrus sinensis*) orange peels. *Biomass Conversion and Biorefinery 13*(6), 5219-5234. https://doi.org/10.1007/s13399-021-01550-6

Yadav, A. M., Nikkam, S., Gajbhiye, P., & Tyeb, M. H. (2017). Modeling and optimization of coal oil agglomeration using response surface methodology and artificial neural network approaches. *International Journal of Mineral Processing 163*, 55-63. https://doi.org/10.1016/j.minpro.2017.04.009

Zheng, X.-Z., Liu, C.-H., & Zhou, H. (2011). Optimization of parameters for microwave-assisted foam mat drying of blackcurrant pulp. *Drying Technology 29*(2), 230-238. https://doi.org/10.1080/07373937.2010.484112

Zielinska, M., Ropelewska, E., & Markowski, M. (2017). Thermophysical properties of raw, hot-air and microwave-vacuum dried cranberry fruits (*Vaccinium macrocarpon*). *Lwt 85*, 204-211. https://doi.org/10.1016/j.lwt.2017.07.016